Assessing Long-Term Trends in Lateral Salt-Marsh Shoreline Change along a U.S. East Coast Latitudinal Gradient

Authors: Burns, Christine J., Alexander, Clark R., and Alber, Merryl

Source: Journal of Coastal Research, 37(2) : 291-301

Published By: Coastal Education and Research Foundation

URL: https://doi.org/10.2112/JCOASTRES-D-19-00043.1

Journal of Coastal Research	37	2	291–301	Coconut Creek, Florida	March 2021

Assessing Long-Term Trends in Lateral Salt-Marsh Shoreline Change along a U.S. East Coast Latitudinal Gradient

Christine J. Burns[†‡], Clark R. Alexander[†‡]*, and Merryl Alber[‡]

[†]Skidaway Institute of Oceanography
University of Georgia
Savannah, GA 31411, U.S.A.

[‡]Department of Marine Sciences
University of Georgia
Athens, GA 30602, U.S.A.

www.cerf-jcr.org

www.JCRonline.org

ABSTRACT

Burns, C.J.; Alexander, C.R., and Alber, M., 2021. Assessing long-term trends in lateral salt-marsh shoreline change along a U.S. East Coast latitudinal gradient. *Journal of Coastal Research*, 37(2), 291–301. Coconut Creek (Florida), ISSN 0749-0208.

Marshes are valuable intertidal habitats that respond to changes in their environment, and their perimeters can rapidly advance or retreat over time. This study used the analyzing moving boundaries using R (AMBUR) tool kit to measure approximately 70 years of edge change at salt marshes within three Long-Term Ecological Research sites along the U.S. East Coast: Georgia Coastal Ecosystems (GCE), Virginia Coast Reserve (VCR), and Plum Island Ecosystems (PIE). At each site, changes were assessed at the open-fetch marsh outer perimeter as well as throughout interior channels of varying sizes. At the open-fetch marsh outer perimeter, both the PIE and VCR study marshes exhibited significant net retreat, with the fastest rates in areas exposed to high fetch where wave action is strong, whereas the GCE marsh exhibited significant net advance. Changes in the sinuous interior channels were smaller, with channels often retreating on one edge but were balanced by advance on the opposite bank. When advance and retreat in the interior channels were considered along with the outer perimeter, the GCE and VCR study marshes exhibited dynamic stability in which overall marsh edge showed no significant net change, and the overall rate of marsh retreat at PIE, although still significant with respect to the uncertainty of the analysis, was considerably reduced. This study demonstrates the importance of assessing shoreline changes throughout the marsh, as rates of retreat and advance at the open-fetch marsh perimeter may differ greatly from those in the interior, and not be indicative of the overall change in marsh edge.

ADDITIONAL INDEX WORDS: *AMBUR, channel order, marsh retreat, marsh advance, channel migration, historical analysis, Long Term Ecological Research.*

INTRODUCTION

Marshes are highly dynamic ecosystems. Although there are feedback mechanisms that allow marshes to establish a vertical equilibrium, they are considered unstable in the horizontal direction (Fagherazzi, 2013; Ganju *et al*., 2017). These systems can experience rapid rates of contraction and expansion in response to external forces (Friedrichs and Perry, 2001; Mariotti, 2020; Sharma *et al*., 2016). In extreme cases, marsh shorelines may change on the order of 10s to 100s of meters per year. For example, Mattheus, Rodriguez, and McKee (2009) showed that forest clearing for silviculture increased sediment input to the Neuse River, North Carolina, resulting in lateral marsh expansion at a rate of over 150 m y^{-1}. The lack of feedback between the processes of advance and retreat results in a marsh that is rarely in horizontal equilibrium; therefore, marsh extent at any given time represents a relatively short-term balance between constructive and destructive processes (Fagherazzi *et al*., 2013).

Studies that measure the advance and retreat of the marsh shoreline often focus on the open-fetch marsh outer perimeter (referred to as "marsh perimeter" throughout this manuscript) which is subject to more wave energy than the marsh interior. Retreat of the marsh perimeter occurs continuously as waves, created by either wind, swell, or boat wakes, break against the exposed muddy shoreline and dislodge sediments (Micheli and Kirchner, 2002; Wallace, Callaway, and Zedler, 2005). As tide levels fall, wave erosion leads to undercutting of the marsh shoreline because the mud unit below the densely vegetated upper marsh is eroded more quickly than the overlying root mat. Marshes exposed to high wave energy tend to be highly scarped and erosional, whereas those in calmer environments tend to be accretional and have more gently sloping shorelines (McLoughlin *et al*., 2015; Sharma *et al*., 2016).

Wave energy as a driver of marsh perimeter retreat has been well documented in marshes throughout the world. In Venice Lagoon, Italy, Marani *et al*. (2011) used dimensional analysis and perimeter retreat data collected from aerial imagery to derive a linear relationship between the rate of volumetric marsh retreat and wave power, which was successfully tested against measured rates of perimeter retreat. In the Gulf of Mexico, Sharma *et al*. (2016) measured short-term changes in marsh shoreline and documented that the shoreline retreated in some years and advanced seaward in others. However, the net effect was ultimately erosional as the environment was too high-energy for revegetation of the slump blocks to occur once separated from the marsh platform.

Interior channels experience advance and retreat of the marsh edge. This process is often seen in sinuous channels, where the edges of meanders can set up a cross-channel current gradient that results in erosion of the outside bank and deposition along the inside (Hughes, 2012; Seminara, 2006). Channels are most stable in densely vegetated marshes, in

DOI: 10.2112/JCOASTRES-D-19-00043.1 received 5 April 2019; accepted in revision 13 September 2020; corrected proofs received 23 November 2020; published pre-print online 29 December 2020.
*Corresponding author: clark.alexander@skio.uga.edu

Figure 1. Location of the three study sites from south to north along the U.S. East Coast: GCE, VCR, and PIE. The GCE and VCR study marshes are 40 km^2 and the PIE study marsh is 21 km^2. Geomorphic setting of creeks and rivers at study sites are shown in Figures 2–4.

those composed of peaty material, and in those with cohesive sediments (Eisma, 1998; Hughes, 2012; Marani *et al.*, 2003).

Sea-level rise (SLR) can also affect the location of the marsh edge. Sea level rose 1.7 mm y^{-1} globally during the 20th century and over 2 mm y^{-1} since the 1990s (Bindoff *et al.*, 2007; Church and White, 2011; Jevrejeva *et al.*, 2008), and these rates are expected to continue accelerating through the latter half of the century. In addition to increasing marsh perimeter erosion as waters rise, SLR affects marsh extent by increasing marsh inundation time beyond that that the vegetation can tolerate (Hartig *et al.*, 2002; Kearney *et al.*, 2002). When the vegetation dies, the marsh shoreline, of both the marsh perimeter and interior channels, becomes more easily eroded and retreats. SLR also increases the water depth in front of the marsh, allowing for the generation of larger waves and faster rates of shoreline retreat along the portion of the marsh perimeter exposed to the increased fetch (Mariotti, 2020; Mariotti and Fagherazzi, 2013). Although waves are a natural force, pervasive erosion of the marsh perimeter can be indicative of an ecosystem stressed by factors such as increased inundation due to SLR (Downs *et al.*, 1994; Eisma, 1998; Hughes, 2012).

This study is a historical analysis of lateral migration of the marsh shoreline at three sites along the U.S. East Coast over the last 70 years. In each case, the present-day marsh edge was compared with historical aerial photographs and National Ocean Service topographic sheets (T-sheets) (Dolan, Fenster, and Home, 1991). Changes were evaluated along the marsh perimeter as well as in the interior channels, and channel order was used to examine the spatial distribution of marsh edge advance and retreat. Understanding how the marsh perimeter and interior channels change over time and across channels of varying sizes provides insight into the dynamic nature of these systems.

Study Sites

Shoreline change was evaluated in salt marshes located in three Long Term Ecological Research Network (LTER) sites on the U.S. East Coast (Figure 1): Georgia Coastal Ecosystems (GCE), Virginia Coast Reserve (VCR), and Plum Island Ecosystems (PIE). LTER sites represent distinct ecosystems around the world and serve as sentinel sites where routine monitoring can identify changes in ecosystem response to natural and anthropogenic forcing. The study marshes represent a gradient of characteristics along a latitudinal gradient, such as varying sediment supply (3 mg L^{-1} to 130 mg L^{-1}), differing dominant vegetation species (*Spartina patens* and *S. alterniflora*), varying rates of relative SLR over the course of the study (2.47 to 3.53 mm y^{-1}), and differing mean tidal ranges (1.2 to 2.9 m; Table 1). Burns, Alber, and Alexander (2020) studied vegetated marsh area change in the GCE, VCR, and PIE study marshes over an approximately 70-year period. They showed that the GCE has maintained total marsh area, the VCR gained total marsh area despite losing marsh area to interior flat expansion, and the PIE has lost marsh area to pond formation and channel widening. The focus of this study was on understanding how the changing dynamics of the perimeter and interior marsh channels influenced marsh extent in these very different settings.

METHODS

Historical aerial photographs and T-sheets produced by the U.S. Coast and Geodetic Survey were used to assess long-term changes in the location of both the marsh perimeter and interior channel edges. Imagery was obtained for three time points at each study site. In all cases high-resolution

Table 1. *Characteristics of the three LTER sites: Georgia Coastal Ecosystems (GCE), Virginia Coast Reserve (VCR), and Plum Island Ecosystems (PIE). Suspended sediment concentrations (SSC) were taken from the literature for each site: GCE (Alber 2018), VCR (Lawson* et al., *2007), and PIE (Drake* et al., *2009; Kirwan* et al., *2010) and cover a range of environments. Relative SLR values were calculated from National Oceanic and Atmospheric Administration tide stations for the length of this study using the PSML database: GCE (#8670870), VCR (#8632200), and PIE (#8443970).*

Site	SSC range (mg L^{-1})	Direction of Strongest Winds	Fetch km	Tidal Range (m)	Relative SLR (mm y^{-1})
GCE	3–130	NE	1.5	2.5	3.00 ± 0.15
VCR	3–48	SSE-SSW N-NE	11	1.2	3.53 ± 0.30
PIE	3–30	N-NE	1.5	2.9	2.47 ± 0.32

Table 2. *Overview of the imagery and T-sheets used in shoreline change analysis. T-sheets were used to extend the record or in place of imagery when suitable imagery was not available.*

Date	Type	Scale	Pixel Size (m)	No. of Photos	% Overlap Between Photos
GCE					
20–22 September 1933	T-sheet	1:10,000	—	1	—
24 November 1933	T-sheet	1:20,000	—	1	—
2 December 1972	Color aerial photograph	1:20,000	1.3	19	50–60% front 50% side
Early 2013	Orthomosaic	—	0.15	—	—
VCR					
2 February 1949	Black and white	1:20,000	0.5	12	50–60% front 30% side
April 1960	T-sheet	1:10,000	—	4	—
Spring 2013	Orthomosaic	—	0.3	—	—
PIE					
1 November 1938	1938 black and white	1:25,000	0.83	5	70% front 40% side
11 June 1971	1971 black and white	1:20,000	1.31	5	20–30% front 10–20% side
April 2013	Orthomosaic	—	0.3	—	—

orthoimagery was available for 2013, and a combination of historical aerial photographs and T-sheets were used for two earlier time points at each site (Table 2). The goal was to have broadly spaced intervals beginning in the 1930s and 1940s with an intermediate data set in the 1970s to compare with the orthoimagery. At GCE, 1933 T-sheets were used for the earliest time point and 1972 aerial photographs for the midpoint. Two sets of aerial photographs were used for PIE, one from 1938 and one from 1971. Finding quality historical data for VCR proved more challenging. A set of 1949 aerial photographs was used for the earliest time point and 1960s T-sheets for the midpoint.

Image Analysis

The imagery was georectified using ground control points (GCPs). Typical GCPs included docks, dock pilings, road intersections, and houses. When discrete GCPs could not be identified, creek and ditch intersections were used (Anders and Byrnes 1991; McLoughlin *et al.*, 2015). Between 10 and 15 GCPs were used for each image, allowing for higher-order polynomial transformations and a better fit (Anders and Byrnes, 1991; Romine *et al.*, 2009).

Once the imagery was georectified, marsh shorelines were digitized adjacent to the main bay or sound (identified as marsh perimeter) as well as along interior channel edges in all imagery using a Wacom Intuos or Wacom Cintiq tablet and ArcGIS 10. A set of rules was established to keep the digitizing process consistent across sites and imagery sources. Imagery collected at low tide was used to reduce the effect of tidal influence on shoreline delineation, and aerial photographs were excluded from analysis if reflection or damage made them difficult to accurately interpret. The shoreline was identified either at the edge of a marsh platform, scarp, or bluff toe in retreating shoreline sections or as the channelward vegetated marsh border or base of vegetated bank in advancing or stable shoreline sections (Crowell, Leatherman, and Buckley, 1991; Pajak and Leatherman, 2002). All shorelines in aerial photographs, T-sheets, and orthoimagery were digitized at a scale of 1:500 to 1:1500. Creeks were delineated down to a 10-m width. Creeks less than 10 m wide were not consistently surveyed on the T-sheets and were often too pixelated in the historical aerial imagery for accurate delineation. As these small creeks can be fairly ephemeral, changes in their morphology are not necessarily indicative of large-scale changes in the location of the marsh edge (Hughes, 2012).

Channel Order

To compare channels with similar drainage characteristics, channels were attributed with their channel order according to the Strahler method (Strahler, 1957) as follows: channels that were the smallest and originated in the marsh were designated as first-order channels. When two first-order channels joined, they formed a second-order channel. This process continued until all the segments were labeled. The total number of channels as well as their distribution and length were assigned within ArcGIS.

First-order channels were often cut off or completely excluded during digitization because they did not meet the minimum size requirement of 10 m. For this reason, first-order channels were not included in the analysis. Both GCE and PIE had sixth-order channels, whereas at VCR fifth order was the highest channel order. This is in part because GCE and PIE marshes drain into a main sixth-order channel, whereas VCR drains into an open bay. The channel order classifications were used to group similar channels for the shoreline change analyses (see below).

Analyzing Moving Boundaries Using R

Analyzing moving boundaries using R (AMBUR) was used to compare the digitized shorelines of both the marsh perimeter and interior channels across time (Jackson, 2017; Jackson, Alexander, and Bush, 2012). The AMBUR package is highly customizable and specifically designed to handle strongly curved features such as marsh and estuarine channels. A baseline was drawn landward and seaward of the digitized shorelines by creating a 5-m buffer around the shoreline shapefile. AMBUR was used to cast transects at 50-m intervals from the outer baseline to the nearest location on the inner baseline. This "near" transect method is designed for curved features because it prevents transects from crossing over each other. A filter was applied to these transects to remove gaps.

The filter uses a moving window average of the azimuths of the five transects within the window to assign a value to the middle transect. AMBUR then uses the intersection of the filtered transects with the digitized shorelines to determine the shoreline change rate.

Rate Calculation Methods

The end-point rate (EPR) method of calculating shoreline change takes the distance of total shoreline movement and divides it by the elapsed time between observations. The EPR method only requires two time points, making it the easiest and most widely used method. For this reason, it is often used in cross-study comparisons (Dolan, Fenster, and Home, 1991). The disadvantage of the EPR approach is that potentially valuable midpoint data are excluded and insights into temporal variation are lost. Since only two data points are used, there is also the potential to give stronger influence to inaccurate data (Dolan, Fenster, and Home, 1991). The linear regression (LRR) method uses a best-fit line through shoreline change rates derived from multiple observations in time. The advantage of this approach is that it uses combinations of all the shorelines to calculate the change rates. The disadvantage is that regressions may give weight to some shorelines over others when shorelines are clustered in time (Dolan, Fenster, and Home, 1991; Jackson, 2005). The difference between EPR and LRR as applied in this study was within the margin of uncertainty associated with the shorelines (see below). Therefore, only the EPR values are discussed here.

Sources of Uncertainty

Shoreline uncertainty values are influenced by the accuracy of the shoreline delineation and digitization, the temporal variability of the shoreline, the number of observations, the proximity of each observation to the time of an actual change in shoreline movement, the period of time between observations, the total time span of the data set, and the method used to calculate shoreline change rate (Dolan, Fenster, and Home, 1991). For this analysis, four main sources of uncertainty were assessed for each shoreline: digitizer consistency, pixel resolution, T-sheet plotting error, and georectification error.

Digitizer consistency (D) was determined for each shoreline by repeatedly digitizing three 1-km shoreline sections five times each. The digitizer consistency differs according to how easy it is to interpret the imagery. To capture this variability, the digitizer consistency was calculated separately for each set of images.

Pixel resolution (P) only applies to the aerial photographs and orthoimagery. Features cannot be resolved if they are smaller than the pixel size.

T-sheet plotting error (T) only applies to T-sheets, which were used at VCR and GCE. Many previous studies have assessed the accuracy of T-sheets, which is dependent on the accuracy of the measuring distance, plane table position, and accurate delineation of the high-water line by the original surveyors (Shalowitz, 1964). The most recent analysis determined that the uncertainty of T-sheet-generated shorelines was ±5.1 m for maps created after 1911 (Romine *et al.*, 2009).

Georectification error (G) is determined using a root mean square error value calculated by the rectification software (in this case ArcGIS). To minimize this error, great care was taken to choose GCPs that were well distributed across the image and were stable over the entire course of the study period.

These four sources of error are random and uncorrelated and thus may be represented by a single measure where the uncertainty (U) of the shoreline position is equal to the square root of the sum of each error source squared (Equation [1]) (Crowell, Leatherman, and Buckley, 1991; Fletcher *et al.*, 2003):

$$U = \pm\sqrt{D^2 + P^2 + T^2 + G^2} \quad (1)$$

This analysis resulted in shoreline positional uncertainties ranging from 1 to 6 m for the various images. Each shoreline was attributed with its uncertainty value, which was incorporated into the combined uncertainty in the subsequent AMBUR analysis. On the basis of the individual uncertainty terms, AMBUR calculates a combined uncertainty value for the rate of change, which incorporates the time span between shoreline ages. Over a 70-year analysis period, total uncertainty decreases in comparison with the uncertainties calculated for individual components of the analysis. The combined uncertainties, applicable to all analyses for each area, were ±0.08 m y^{-1} for GCE, ±0.06 m y^{-1} for VCR, and ±0.06 m y^{-1} for PIE. Unless otherwise stated, the analysis was confined to transects that exceeded these values, where the calculated EPR was greater than the uncertainty.

RESULTS

The AMBUR analysis was used to estimate shoreline change over the entire study marsh at each of the three LTER sites. Results were also grouped by channel order, which allowed for the evaluation of how patterns of advance and retreat change with channel size and to separate the marsh perimeter from interior channels.

Georgia Coastal Ecosystems

The EPR analysis of GCE marsh shorelines was calculated on the basis of shorelines from 1933 and 2013 (80 y), which yielded a total uncertainty of ±0.08 m y^{-1} for all transects in the GCE. There were 1935 transects, and of these transects, 1477 (74%) experienced change greater than the uncertainty. In this section, the results are based on these 1477 transects that show change greater than the uncertainty. Across the entire site, 49% of transects were retreating and 51% were advancing over the study period (Table 3). The maximum rate of marsh advance at GCE was two times faster than the maximum rate of retreat. The fastest rates of advance largely occurred at the southern tip of Rock Island (Figure 2), whereas the fastest rates of retreat were observed along Hudson Creek and the NE side of Rock Island. The mean EPR for the entire study site was +0.04 m y^{-1}, which was less than the uncertainty.

The GCE had 5.5 km of linear marsh along the marsh perimeter, with a mean EPR of +0.23 m y^{-1} (35% of transects retreating, 65% advancing) (Table 3). The mean EPR of advancing transects was twice as fast as that of retreating transects; the maximum EPR of advancing transects was over +3.0 m y^{-1}, whereas the maximum rate of retreat was –0.42 m y^{-1}. Most of the retreat at the marsh perimeter was concentrated in the NE corner of Rock Island. There were

Table 3. *AMBUR transect data for study marshes at each LTER site. Analysis was conducted only on transects where change was greater than the uncertainty (column 3). Data are presented for each channel order as well as for the entire study area. Mean rates greater than the uncertainty for each group and study area are shown in bold. The error for GCE was ±0.08 m y^{-1}, for VCR was ±0.06 m y^{-1}, and for PIE was ±0.06 m yr^{-1}. The end-point rate of change (EPR) was calculated using the AMBUR package in R.*

Channel Order	No. of Transects	No. of Transects > Uncertainty	Retreating Transects %	Retreating Transects Mean EPR (m y^{-1})	Retreating Transects Max EPR (m y^{-1})	Advancing Transects %	Advancing Transects Mean EPR (m y^{-1})	Advancing Transects Max EPR (m y^{-1})	Overall Mean EPR (m y^{-1})
GCE									
2	375	276	49	**−0.25**	**−1.47**	51	**+0.30**	**+1.23**	+0.03
3	585	442	35	**−0.24**	**−1.11**	65	**+0.36**	**+3.00**	**+0.15**
4	641	505	57	**−0.35**	**−1.69**	43	**+0.36**	**+1.46**	−0.04
5	235	189	69	**−0.36**	**−0.77**	31	**+0.57**	**+3.08**	−0.07
6	99	65	35	**−0.21**	**−0.42**	65	**+0.47**	**+3.03**	**+0.23**
Total	1,935	1,477	50	**−0.30**	**−1.69**	50	**+0.37**	**+3.08**	+0.04
VCR									
2	406	328	50	**−0.18**	**−1.23**	50	**+0.22**	**+0.60**	+0.02
3	474	414	46	**−0.17**	**−0.92**	54	**+0.27**	**+0.81**	**+0.07**
4	294	273	25	**−0.21**	**−0.56**	75	**+0.49**	**+2.10**	**+0.31**
5	34	28	57	**−0.24**	**−1.00**	32	**+0.16**	**+0.43**	**−0.07**
Marsh perimeter	321	292	69	**−0.61**	**−2.21**	31	**+0.66**	**+3.62**	**−0.21**
Total	1,529	1335	48	**−0.32**	**−2.21**	52	**+0.37**	**+3.62**	**+0.04**
PIE									
2	443	147	76	**−0.10**	**−0.11**	24	**+0.10**	**+0.13**	−0.05
3	353	181	92	**−0.13**	**−0.25**	8	**+0.12**	**+0.31**	**−0.11**
4	213	154	88	**−0.18**	**−0.88**	12	**+0.40**	**+1.81**	**−0.11**
5	199	135	61	**−0.21**	**−0.75**	32	**+0.19**	**+0.81**	**−0.08**
6	61	58	95	**−0.32**	**−0.61**	5	**+0.18**	**+0.34**	**−0.29**
Total	1,269	675	83	**−0.17**	**−0.88**	17	**+0.19**	**+1.81**	**−0.11**

Figure 2. AMBUR-produced transects of shoreline change at the GCE study site. The lengths of transects represent the magnitude of change from 1933 to 2013. The color of the transects indicates whether the transects were advancing (blue) or retreating (red). When the rate of change was less than the uncertainty, the transects are listed as "no change" (gray). The inset demonstrates the coupled patterns of advance and retreat found in the lower-order channels.

95.7 km of interior channel edge. In contrast to the marsh perimeter, retreating and advancing transects in the interior channels were balanced (50% of transects retreating, 50% advancing) and the mean EPR was only +0.04 m y^{-1}. The mean EPR of channels ranged from −0.07 m y^{-1} (for fifth-order channels) to +0.15 m y^{-1} (for second-order channels; Table 3). Second- and third-order channels often exhibited a pattern of retreating and advancing transects along a channel edge, which alternated along the bank as the channel meandered (Figure 2, inset), whereas the transects on the opposing bank showed a complementary pattern of retreat and advance. Of the interior channels, only third-order channels had a mean EPR that was greater than the uncertainty term. Sixty-five percent of the third-order channel transects advanced, and the mean EPR was +0.15 m y^{-1}. Unlike the lower-order channels that experienced retreat and advances on both banks, half of the fourth-order channels experienced uniform change, all greater than the uncertainty. For example, Hudson Creek widened as both banks retreated, and the Carnigan River narrowed as the marsh on both sides advanced. Fifth-order channels had the highest percentage of retreating transects (69%) at GCE, yet the mean EPR remained slow (−0.07 m y^{-1}). This slow, retreating EPR resulted from averaging of fast rates (over +3.0 m y^{-1}) of marsh advance occurring at the southern edge of Rock Island, which offset the more numerous but more slowly retreating transects along the channel.

Virginia Coastal Reserve

At VCR the EPR comparison was between shorelines from 1949 and 2013 (64 y; Figure 3), which yielded a total uncertainty of ±0.06 m y^{-1} for all transects in the VCR. Of 1529 transects, 1335 (87%) experienced change greater than the uncertainty. In this section, the results are based on these

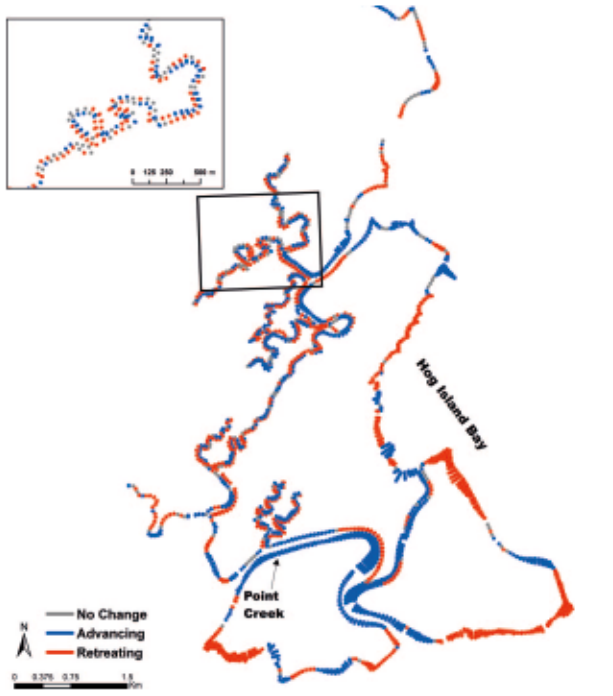

Figure 3. AMBUR-produced transects of shoreline change at the VCR study site. The lengths of transects represent the magnitude of change from 1949 to 2013. The color of the transects indicates whether transects were advancing (blue) or retreating (red). When the rate of change was less than the uncertainty, transects are listed as "no change" (gray). The inset demonstrates the coupled patterns of erosion and accretion found in the lower-order channels.

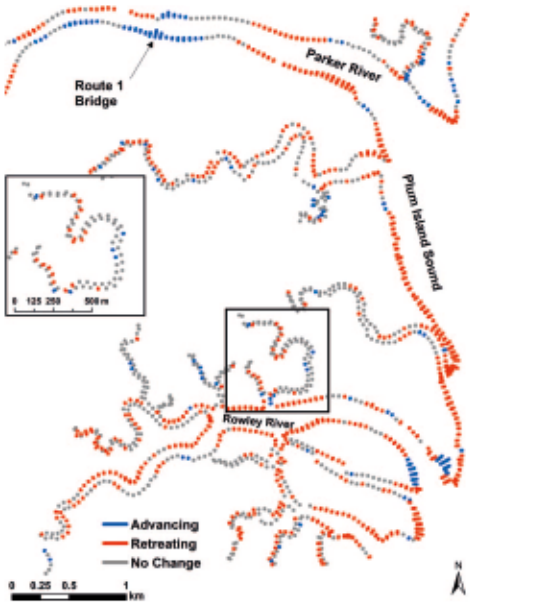

Figure 4. AMBUR-produced transects of shoreline change at the PIE study site. The length of transects represents the magnitude of change from 1938 to 2013. The color of the transects indicates whether the transects were advancing (blue) or retreating (red). When the rate of change was less than the uncertainty, the transects are listed as "no change" (gray). Unlike the other two sites, patterns of erosion and accretion are less clear in the lower-order channels (inset).

1335 transects that show change greater than the uncertainty. Of these transects, 50% were retreating and 50% were advancing (Table 3). The mean overall EPR for the entire site, +0.04 m y^{-1}, was smaller than the uncertainty. The fastest rates of retreat at VCR occurred along the marsh perimeter adjacent to Hog Island Bay, and the fastest rates of marsh advance occurred along Point Creek (Figure 3).

VCR had the longest marsh perimeter of the three sites, with 15.9 km of linear marsh and a mean EPR of –0.21 m y^{-1} (±0.06 m y^{-1}; 69% transects retreating, 31% advancing). These marsh perimeter transects were dominated by retreat and accounted for 22% of all transects analyzed at VCR. The small segments of perimeter marsh that were advancing were observed behind remnants of small marsh islands.

The VCR interior channel edges comprised 63.5 km of marsh shoreline; 86% of transects had EPR values greater than the uncertainty (57% of transects advancing and 43% retreating). The mean EPR for interior transects was 0.10 m y^{-1} ±0.06 m y^{-1}. The mean EPR values of all channel orders were greater than the uncertainty term except in second-order channels (Table 3). Similarly to GCE, the patterns of marsh advance and retreat alternated along the length of the channels as they meandered through the marsh (Figure 3 inset). The fourth-order channel, Point Creek, was an exception, as the marsh on both banks advanced rapidly at over +2.0 m y^{-1}. Here, marsh advance on the inside of a sharp meander resulted in the connection of a point bar with the interior marsh edge. This point bar became vegetated, rapidly extending the marsh platform by almost 100 m in some locations. Fifth-order channels were a very small portion of the extant channels, and in general exhibited relatively slow, retreating EPRs.

Plum Island Ecosystems

At PIE, the EPR comparison was between shorelines from 1938 and 2013 (75 y), which yielded a total uncertainty of ±0.06 m y^{-1} for all transects in PIE. Of 1269 transects, only 675 (53%) experienced change outside of the uncertainty. In this section, the results are based on these 675 transects that show change greater than the uncertainty. Of these transects, 83% were retreating and 17% were advancing. The magnitude of advance and retreat rates was much smaller at PIE than at the other two sites, and the overall, site-wide EPR value was negative but still greater than the uncertainty, –0.11 m y^{-1} ± 0.06 m y^{-1}. The fastest rates of marsh retreat were found along Plum Island Sound, whereas the fastest rates of marsh advance occurred along the Parker River (Figure 4; Table 3).

PIE had 3.4 km of linear perimeter marsh and had a mean EPR of –0.29 m y^{-1} (95% transects retreating and 5% advancing). The interior marsh channels contained 65.0 km of marsh edge, where 82% of transects were retreating and 18% were advancing, resulting in an interior channel EPR of –0.09 m y^{-1}.

When evaluated by channel order, the channel EPRs ranged from –0.05 m y^{-1} (for second-order channels) to –0.11 m y^{-1} (for third- and fourth-order channels) (Table 3). Because the

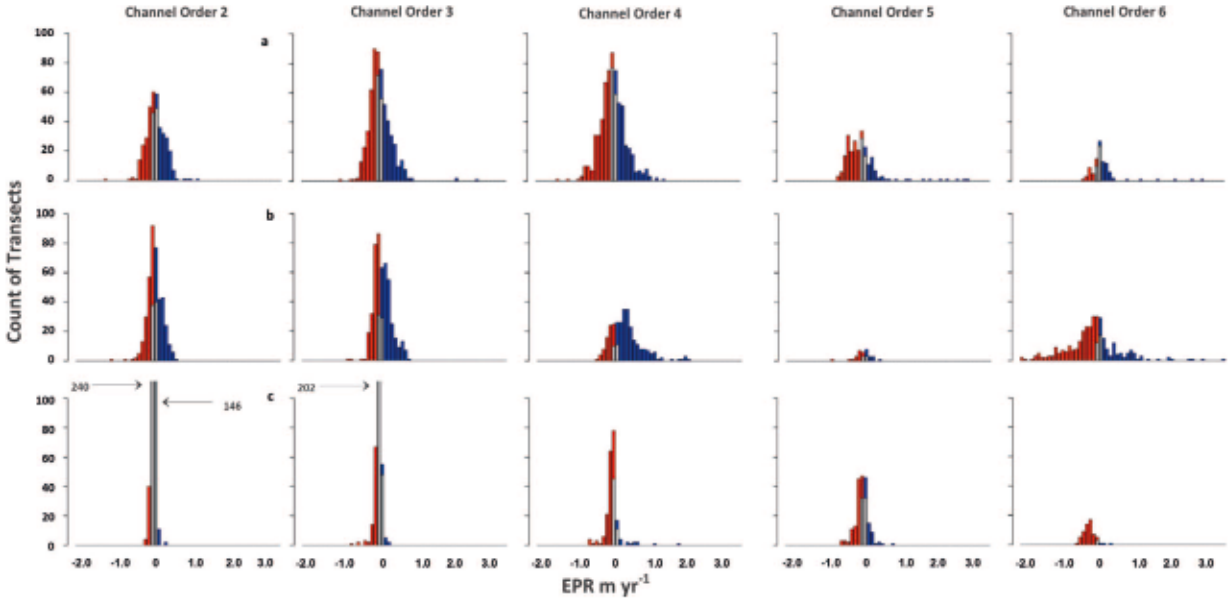

Figure 5. Histograms showing the frequency of EPR values in 0.1 m y^{-1} bins for each channel order at (a) GCE, (b) VCR, and (c) PIE. Gray bars indicate EPR values within the uncertainty of the analysis, red bars indicate shoreline retreat, and blue bars indicate shoreline advance. The number of second- and third-order channels at PIE are indicated to maintain equivalent x and y axes across all three study sites.

transects exhibiting retreat dominated the interior marsh channels, PIE lacked the distinct, alternating patterns associated with meandering channels as documented at GCE and VCR (Figure 4 inset). All channel orders had greater amounts of retreating transects (between 61 and 95%) and the negative EPR values of all channel orders were greater than the uncertainty except for second-order channels. Fifth-order channels exhibited the lowest percentage of transects, indicating retreat (65%). The Parker River was the main fifth-order channel included at this site. It had an extensive advancing area near the Route 1 Bridge (Figure 4). During the course of this study, a large marina was constructed on the southern end of the bridge, which likely caused sedimentation and marsh advance in that area.

Intra- and Cross-Site Comparisons

The marsh perimeter showed greater rates of change than the interior channel margins at all three sites; however, it represented only a small portion of these marshes. When both the marsh perimeter and interior channel margins were assessed as a whole, PIE was the only site where the mean EPR for the entire study area was negative and was greater than the uncertainty in the analysis, –0.11 m y^{-1} ± 0.06 m y^{-1} (Table 3). The overall mean EPRs for both GCE and VCR study sites were positive, but within the uncertainty. The EPR of individual transects exhibited a much greater range in both rates of retreat and advance at GCE and VCR, whereas at PIE they were consistently slow and exhibited a much narrower distribution, with only 53% of transects exhibiting rates greater than the uncertainty (Figure 5). VCR had the largest extremes, with both the fastest rates of shoreline retreat and the fastest rates of shoreline advance.

The frequency distributions of EPR values for all transects evaluated in this study showed an increasing range of values with increasing channel order at all three sites, and the standard deviation of the mean EPR values increased similarly, indicating an increase in the magnitude of change, and probably forcing, in larger channels (Figure 5, Table 4). In many cases distributions were skewed to the right, with long tails in the higher-order channels (*e.g.*, fifth- and sixth-order channels at GCE; Table 4). However, there were a few cases where they were skewed left (*e.g.*, third-order channels at PIE

Table 4. *Descriptive statistics for histograms showing the distribution of all transect EPR values determined in this study (shown in Figure 5). Letters denote study site and numbers denote channel order.*

	Mean (m y^{-1})	Standard Deviation (m y^{-1})	Skewness (statistic)
GCE 2	0.02	0.28	0.09
GCE 3	0.12	0.35	1.99
GCE 4	–0.04	0.38	0.24
GCE 5	–0.06	0.55	3.15
GCE 6	0.16	0.54	3.74
Full site	0.03	0.40	1.91
VCR 2	0.02	0.22	–0.39
VCR 3	0.06	0.25	0.42
VCR 4	0.29	0.46	1.30
VCR 5	–0.05	0.25	–1.57
VCR 6	–0.19	0.79	0.75
Full site	0.04	0.48	0.39
PIE 2	–0.02	0.07	0.32
PIE 3	–0.07	0.11	–2.82
PIE 4	–0.09	0.24	2.88
PIE 5	–0.06	0.20	0.19
PIE 6	–0.28	0.17	0.88
Full site	–0.06	0.16	1.16

Table 5. *Pairwise comparison of the three sites using the nonparametric Kruskal–Wallis test. Asymptotic significance is reported when N is large (>30), as in this analysis. The adjusted significance uses the Bonferroni correction for multiple tests. Both significance values indicate that PIE is statistically different from GCE and VCR.*

	Test Statistic	Std. Error	Std. test Statistic	Significance	Adjusted Significance
PIE – GCE	387.02	49.36	7.84	<0.01	<0.01
PIE – VCR	−497.08	51.89	−9.58	<0.01	<0.01
GCE – VCR	−110.07	46.76	−2.35	0.02	0.06

and fifth-order channels at VCR). Note that these analyses include transects with EPRs that are less than the uncertainty values because values close to zero net change over ~70 years and within the measurement error still represent real, albeit small, absolute changes. Because the data do not meet assumptions of normality, a nonparametric Kruskal–Wallis test (Kruskal, 1952) was performed to test whether the rates of shoreline change are different at all three sites. The results of this test indicated that the three sites are statistically different ($H = 99.93$, 2 df, $p < 0.01$). A pairwise comparison reveals that PIE was different from both GCE and VCR, whereas the differences between GCE and VCR were not statistically significant (Table 5).

DISCUSSION

This study analyzed long-term changes in the positions of the marsh perimeter and interior channels at three locations along the U.S. East Coast to provide insight into lateral changes in marsh extent over the past ~70 years. Although there is inherent uncertainty associated with using historical maps, the imagery used in this study met the 60-year minimum for long-term analysis recommended by Crowell, Leatherman, and Buckley (1993). This minimum standard for shoreline analysis is a way to decrease the uncertainty associated with using historical data sets and increase the confidence of the estimated rates of change. The study was mostly confined to analyses of transects that exhibited changes that were greater than the uncertainty for each study area.

Two of the sites evaluated, GCE and VCR, exhibited dynamic stability in which high rates of both advance and retreat in the marsh perimeter and channel edges occurred that in aggregate resulted in little net change. The third site, PIE, lacked the dynamism of the other two sites, and showed net retreat. The highest rates of change were generally observed along the marsh perimeter as compared with the interior channel edges, with the marsh perimeter retreating at VCR (–0.21 m y^{-1}) and PIE (–0.29 m y^{-1}) and advancing at GCE (+0.23 m y^{-1}) over the last approximately 70 years. These rates of change are on the lower end of those previously reported from the literature for the U.S. East Coast. Studies of change of the marsh perimeter at sites surrounding Hog Island Bay, Virginia (McLoughlin *et al.*, 2015), coastal Georgia (Jackson, Alexander, and Bush, 2012), and Rehoboth Bay, Delaware (Schwimmer, 2001) reported retreat rates spanning –0.02 to –7.3 m y^{-1}.

The locations of areas with retreating marsh perimeter at both PIE and VCR suggest that wind-wave energy may be an important factor driving lateral marsh retreat at these sites. At VCR the winds average 7.5 m s^{-1} overall, but the NNE winds associated with winter storms are the strongest, commonly exceeding >15 m s^{-1} (Fagherazzi and Wiberg, 2009; Table 1). The VCR study marsh juts out into the open lagoon of Hog Island Bay, creating a shoreline oriented toward the NE, with a fetch that ranges from 8 to 11 km, and to the south and SE. The highest rates of retreat were observed on the exposed NE shoreline, whereas the sheltered southern shore of the peninsula exhibits slower retreat rates and, in some areas, marsh advance.

Much of the perimeter marsh of PIE is roughly linear and faces east. The dominant winds at this site are from the west, but as at VCR, the strongest winds are from the NE, often exceeding 17.5 m s^{-1} (Fagherazzi *et al.*, 2014). Because this entire east-facing shoreline receives similar wind-wave energy, the rate of retreat was spatially consistent. The fetch across Plum Island Sound from the NE is only about 1.5 km; in addition, there are large shoals in the sound that reduce the fetch to less than 0.5 km as the tide falls. This likely explains why the fastest rates of retreat along Plum Island Sound (PIE) are 1 m y^{-1} less than those documented along Hog Island Bay at the VCR. This also suggests that at PIE, the impact of wind waves at the eastward-facing marsh perimeter may be tidally dependent.

In contrast, the GCE exhibited shoreline advance along much of the marsh perimeter. Although the strongest winds come from the NE, they are seasonally limited and the fetch is less than 1–2 km (Di Iorio and Castelao, 2013; Weber and Blanton, 1980). In addition to the lower fetch, the high input of sediment at this study site may have contributed to the observed advance of the marsh perimeter (Table 1).

Rates of channel edge migration in the marsh interior were generally much slower than the rates of change of the marsh perimeter at all sites, with a pattern of decreasing EPR in lower-order channels. EPRs showed retreat for all orders of interior channels at PIE, whereas at GCE and VCR the lower-order channel edges advanced. These results align with observations that marsh channels have widened at PIE, causing a loss of marsh based on GIS analysis of marsh feature distributions (Burns *et al.*, 2020). Published rates of interior channel migration range from approximately 0.2 m y^{-1} to 0.9 m y^{-1} in both microtidal (Delaware Bay [Garofalo, 1980]; Venice Lagoon, Italy [Finotello *et al.*, 2018; Rizzeto and Tosi, 2012]) and mesotidal (San Francisco Bay [Gabet, 1998]; Long Island, New York [Browne, 2017]) settings. In this study, migration rates of individual channels were highly variable and ranged from 0.02 to 0.31 m y^{-1}. These rates are similar to published rates, although previous studies did not provide channel-order data and thus it is difficult to compare these results. One short-term study in the mesotidal salt marshes of Georgia (Letzsch and Frey, 1980) showed high rates of channel migration in third-order channels (2–4 m y^{-1}), but the study period was short (<2 y) and these results probably do not reflect the long-

term (~70 y) trends assessed in this study. With the advent of inexpensive methods (*i.e.* drones) to collect high-resolution, high-frequency image data of tidal creek behavior, short-term channel migration studies will be logistically and methodologically more straightforward, providing insight into these timescale issues (Kim *et al.*, 2019; Taddia, Stecchi, and Pellegrinelli, 2019).

The slow retreat of interior channel margins at PIE may be due to differences in vegetation. GCE and VCR are dominated by the low marsh grass, *S. alterniflora*, whereas PIE is largely vegetated with the denser-growing high marsh grass, *S. patens*. More densely growing vegetation and thick root masses stabilize the marsh by dissipating flows, binding sediments, and slowing erosion (Gabet, 1998; Lawrence, Allen, and Havelock, 2004; Micheli and Kirchner, 2002), which may make them less susceptible to retreat. PIE interior channel margins retreated slowly on both channel banks, at rates ~0.1 m y^{-1}, whereas GCE and VCR exhibited EPR rates faster than those observed at PIE, often times with one bank retreating and the opposite bank advancing at rates 2–10× as fast (*e.g.*, Letzsch and Frey, 1980).

Within each marsh interior site, the spatial distribution of retreating and advancing transects was influenced by the sinuous nature of marsh channels. Retreating and advancing transects along a single shoreline alternated as the channel migrated through the marsh. Cross-channel patterns of advance and retreat, which maintain channel width as retreat of one side of the channel is accommodated by advance of the opposite side, has been previously documented in first- through third-order channels in short-term studies of the Duplin River and Blackbeard Creek, Georgia (Letzch and Frey, 1980; Wadsworth, 1980). In this study, the total rate of shoreline change, and total shoreline change as well, for similar-order channels were often close to zero net change because the retreating and advancing transects sum to zero.

CONCLUSIONS

Many studies look at positional changes of the marsh perimeter, or they look at patterns of interior channel migration, widening, or narrowing, but rarely both at once (*e.g.*, Eulie *et al.*, 2016; Gabet, 1998; Letzsch and Frey, 1980; Mariotti, 2018; McLoughlin *et al.*, 2015; Schwimmer, 2001; Wilson *et al.*, 2014). Furthermore, many channel migration studies only study a select number and size of channels rather than a full range of sizes. The different channels found in different areas of the marsh are likely to respond to different processes, with wind-wave energy being important for modifying exposed marsh perimeters, which are by definition more exposed to open fetch and channel meandering affecting the spatial pattern of shoreline change in the smaller interior channels. However, shoreline change affects channels of all sizes and this study shows the value of including both of these marsh environments in assessing overall rates of shoreline change in marshes, and with implications for total marsh areal change and in predicting future trajectories.

When just evaluating the exposed marsh perimeter, the marsh shorelines at VCR and PIE exhibited net retreat and that at GCE exhibited net advance. However, 95, 79, and 95% of transects fell within the marsh interior at GCE, VCR, and PIE, respectively. When shoreline positional change rates in these interior channels were included, the GCE and VCR did not show an overall net shoreline positional change greater than the uncertainty across the approximately 70-year study period. Although PIE showed net overall retreat when the entire marsh shoreline change was evaluated, the overall rate was considerably slower than when just the marsh perimeter was considered. Ultimately, it is important to look at both marsh components (marsh perimeter and interior channel edges) when assessing marsh shoreline change to capture the full magnitude of positional shoreline change in these systems.

Marshes are naturally dynamic systems, and lateral marsh change is not necessarily a sign of long-term change in marsh area. Both the GCE and VCR marshes experienced fast rates of retreat and advance along the marsh shoreline, but again these processes balanced throughout the marsh and neither site showed net change. At PIE, which did show net retreat, the range of EPRs was considerably smaller than at the other two sites. However, it is possible that processes that act to prolong inundation or increase wind-wave erosion such as SLR or increased storminess may affect future shoreline change at these sites.

ACKNOWLEDGMENTS

We thank Mike Robinson, John Porter, Matt Kirwan, and Hap Garritt for providing the imagery used in this study and Marguerite Madden and Charles Hopkinson for comments on the manuscript. This research was supported by the National Science Foundation-funded Coastal SEES (NSF14-26308) and Georgia Coastal Ecosystems LTER (OCE12-37140; OCE18-32178) projects.

LITERATURE CITED

Alber, M., 2018. Long-term water quality monitoring in the Altamaha, Doboy and Sapelo sounds and the Duplin River near Sapelo Island, Georgia from November 2013 to December 2015. Georgia Coastal Ecosystems LTER Project, University of Georgia, Long Term Ecological Research Network. http://dx.doi.org/10.6073/pasta/c55e5b0e279ea54151517cabe894a44b

Anders, F.J. and Byrnes, M.B., 1991. Accuracy of shoreline change rates as determined from maps and aerial photographs. *Shore and Beach*, 59(1), 17–26.

Bindoff, N.L.; Willebrand, J.; Artale, V.; Cazenave, A.; Gregory, J.; Gulev, S.; Hanawa, K.; Le Quéré, C.; Levitus, S.; Nojiri, Y.; Shum, C.K.; Talley, L.D., and Unnikrishnan, A., 2007. Observations: Oceanic climate change and sea level. *In:* Solomon, S.; Qin, D.; Manning, M.; Chen, Z.; Marquis, M.; Averyt, K.B.; Tignor, M., and Miller, H.L. (eds), *Climate Change 2007: The Physical Science Basis. Contribution of Working Group I to the Fourth Assessment Report of the Intergovernmental Panel on Climate Change*. Cambridge: Cambridge University Press.

Browne, J.P., 2017. Long-term erosional trends along channelized salt marsh edges. *Estuaries and Coasts*, 40(6), 1566–1575.

Burns, C.; Alber, M., and Alexander, C., 2020. Historical changes in the vegetated area of salt marshes. *Estuaries and Coasts*, https://doi.org/10.1007/s12237-020-00781-6

Church, J.A. and White, N.J., 2011. Sea-level rise from the late 19th to the early 21st century. *Surveys in Geophysics*, 32(4–5), 585–602.

Crowell, M.; Leatherman, S.P., and Buckley, M.K., 1991. Historical shoreline change: Error analysis and mapping accuracy. *Journal of Coastal Research*, 7(3), 839–852.

Crowell, M.; Leatherman, S.P., and Buckley, M.K., 1993. Shoreline change rate analysis: Long term versus short term data. *Shore and Beach*, 61(2), 13–20.

Di Iorio, D. and Castelao, R.M., 2013. The dynamical response of salinity to freshwater discharge and wind forcing in adjacent estuaries on the Georgia coast. *Oceanography*, 26(3), 44–51.
Dolan, R.; Fenster, M., and Home, S.J., 1991. Temporal analysis of shoreline recession and accretion. *Journal of Coastal Research*, 7(3), 723–744.
Downs, L.L.; Nicholls, R.J.; Leatherman, S.P., and Hautzenroder, J., 1994. Historic evolution of a marsh island: Bloodsworth Island, Maryland. *Journal of Coastal Research*, 10(4), 1031–1044.
Drake, D.C.; Peterson, B.J.; Galvan, K.A.; Deegan, L.A.; Hopkinson, C.; Johnson, J.M.; Koop-Jakobsen, K.; Lemay, L.E., and Picard, C., 2009. Salt marsh ecosystem biogeochemical responses to nutrient enrichment: A paired ^{15}N tracer-study. *Ecology*, 90(9), 2535–2546.
Eisma, D., 1998. *Intertidal Deposits: River Mouths, Tidal Flats, and Coastal Lagoons*. Boca Raton, Florida: CRC Press. 525p.
Eulie, D.O.; Walsh, J.P.; Corbett, D.R., and Mulligan, R.P., 2016. Temporal and spatial dynamics of estuarine shoreline change in the Albemarle–Pamlico estuarine system, North Carolina, USA. *Estuaries and Coasts*, 40(3), 1–17.
Fagherazzi, S., 2013. The ephemeral life of a salt marsh. *Geology*, 41(8), 943–944.
Fagherazzia, S.; Mariottia, G.; Banks, A.T.; Morgan, E.J., and Fulweiler, R.W., 2014. The relationships among hydrodynamics, sediment distribution, and chlorophyll in a mesotidal estuary. *Estuarine, Coastal and Shelf Science*, 144, 54–64.
Fagherazzi, S.; Mariotti, G.; Wiberg, P.L., and McGlathery, K.J., 2013. Marsh collapse does not require sea level rise. *Oceanography*, 26(3), 70–77.
Fagherazzi, S. and Wiberg, P.L., 2009. Importance of wind conditions, fetch, and water levels on wave-generated shear stresses in shallow intertidal basins. *Journal of Geophysical Research: Earth Surface*, 114(F03022), 1–12.
Finotello, S.; Lanzoni, S.; Ghinassi, M.; Marani, M.; Rinaldo, A., and D'Alpaos, A., 2018. Field migration rates of tidal meanders recapitulate fluvial morphodynamics. *Proceedings of the National Academy of Sciences of the United States of America*, 115 (7), 1463–1468.
Fletcher, C.; Rooney, J.; Barbee, M.; Lim, S.C., and Richmond, B., 2003. Mapping shoreline change using digital orthophotogrammetry on Maui, Hawaii. *In:* Byrnes, M.B.; Crowell, M., and Fowler, C. (eds.), *Shoreline Mapping and Change Analysis Technical Considerations and Management Implications. Journal of Coastal Research*, Special Issue No. 38, pp. 106–124.
Friedrichs, C.T. and Perry, J.E., 2001. Tidal salt marsh morphodynamics: A synthesis. *In:* Goodwin, P. and Mehta, A.J. (eds), *Tidal Wetland Physical and Ecological Processes. Journal of Coastal Research*, Special Issue No. 27, pp. 7–37.
Gabet, E.J., 1998. Lateral migration and bank erosion in a salt marsh tidal channel in San Francisco Bay, California. *Estuaries*, 21(4), 745–753.
Ganju, N.; Defne, Z.; Kirwan, M.L.; Fagherazzi, S.; D'Alpaos, A., and Caniello, L., 2017. Spatially integrative metrics reveal hidden vulnerability of microtidal salt marshes. *Nature Communications*, 8, 14156.
Garofalo, D., 1980. The influence of wetland vegetation on tidal stream channel migration and morphology. *Estuaries*, *3*(4), 258–270.
Hartig, E.K.; Gornitz, V.; Kolker, A.; Mushacke, F., and Fallon, D., 2002. Anthropogenic and climate-change impacts on salt marshes of Jamaica Bay, New York City. *Wetlands*, 22(1): 71–89.
Hayden, B.P. and Hayden, N.R., 2003. Decadal and century-long changes in storminess at long-term ecological research sites. *In:* Greenland, D.; Goodin, D.G., and Smith, R.C. (eds), *Climate Variability and Ecosystem Response at Long-Term Ecological Research Sites*. New York: Oxford University Press, pp. 262–285.
Hughes, Z.J., 2012. Tidal channels on tidal flats and marshes. *In:* Davis, R.A, Jr. and Dalrymple, R.W. (eds.), *Principles of Tidal Sedimentology*. Dordrecht, The Netherlands: Springer, pp. 269–300.
Jackson, C.W., 2017. Ambur: Analyzing moving boundaries using R (R package version 1.1.26/r278). https://R-Forge.R-project.org/projects/ambur/
Jackson, C.W., 2005. Quantitative shoreline change analysis of and inlet-influenced transgressive barrier system: Figure Eight Island, North Carolina. Wilmington, North Carolina: University of North Carolina, Master's thesis, 95p.
Jackson, C.W.; Alexander, C.R., and Bush, D.M., 2012. Application of the AMBUR R package for spatio-temporal analysis of shoreline change: Jekyll Island, Georgia, USA. *Computers & Geosciences*, 41, 199–207.
Jevrejeva, S.; Moore, J.C.; Grinsted, A., and Woodworth, P.L., 2008. Recent global sea level acceleration started over 200 years ago? *Geophysical Research Letters*, 35(8), L08715.
Kearney, M.S.; Rogers, A.S.; Townshend, J.R.; Rizzo, E.; Stutzer, D.; Stevenson, J.C., and Sundborg, K., 2002. Landsat imagery shows decline of coastal marshes in Chesapeake and Delaware Bays. *Eos, Transactions American Geophysical Union*, 83(16), 173–178.
Kim, S.; Park, S.; Han, J.; Son, S.; Lee, S.; Han, K.; Kim, J., and Kim J., 2019. Feasibility of UAV photogrammetry for coastal monitoring: A case study in Imlang Beach, South Korea. *In: Advances in Remote Sensing and Geoscience Information Systems of Coastal Environments Journal of Coastal Research*, Special Issue No. 90, pp. 386–392.
Kirwan, M.L.; Guntenspergen, G.R.; D'Alpaos, A.; Morris, J.T.; Mudd, S.M., and Temmerman, S., 2010. Limits on the adaptability of coastal marshes to rising sea level. *Geophysical Research Letters*, 37(23), L23401.
Kruskal, W., 1952. Use of ranks in one-criterion variance analysis. *Journal of the American Statistical Association*, 47(260), 583–621.
Lawrence, D.S.; Allen, J.R., and Havelock, G.M., 2004. Salt marsh morphodynamics: An investigation of tidal flows and marsh channel equilibrium. *Journal of Coastal Research*, 20(1), 301–316.
Lawson, S.E.; Wiberg, P.L.; McGlathery, K.J., and Fugate, D.C., 2007. Wind-driven sediment suspension controls light availability in a shallow coastal lagoon. *Estuaries and Coasts*, 30(1), 102–112.
Letzsch, W.S. and Frey, R.W., 1980. Erosion of salt marsh tidal creek banks, Sapelo Island, GA. *Senckenbergiana Maritima*, 12(5/6), 201–212.
Marani, M.; Belluco, E.; D'Alpaos, A.; Defina, A.; Lanzoni, S., and Rinaldo, A., 2003. On the drainage density of tidal networks. *Water Resources Research*, 39(2), 1040.
Marani, M.; D'Alpaos, A.; Lanzoni, S., and Santalucia, M., 2011. Understanding and predicting wave erosion of marsh perimeters. *Geophysical Research Letters*, 38(21), L21401.
Mariotti, G., 2018. Marsh channel morphological response to sea level rise and sediment supply. *Estuarine, Coastal, and Shelf Science*, 209, 89–101.
Mariotti, G., 2020. Beyond marsh drowning: The many faces of marsh loss (and gain). *Advances in Water Resources*, 144(2020), 103710.
Mariotti, G. and Fagherazzi, S., 2013. Critical width of tidal flats triggers marsh collapse in the absence of sea-level rise. *Proceedings of the National Academy of Sciences of the United States of America*, 110(14), 5353–5356.
Mattheus, C.R.; Rodriguez, A.B., and McKee, B.A., 2009. Direct connectivity between upstream and downstream promotes rapid response of lower coastal-plain rivers to land-use change. *Geophysical Research Letters*, 36(20). doi: 10.1029/2009GL039995
McLoughlin, S.M.; Wiberg, P.L.; Safak, I., and McGlathery, K.J., 2015. Rates and forcing of marsh edge erosion in a shallow coastal bay. *Estuaries and Coasts*, 38(2), 620–638.
Micheli, E.R. and Kirchner, J.W., 2002. Effects of wet meadow riparian vegetation on streambank erosions. 2. Measurements of vegetated bank strength and consequences for failure mechanics. *Earth Surface Processes and Landforms*, 27, 687–697.
Pajak, M. and Leatherman, S., 2002. The high water line as shoreline indicator. *Journal of Coastal Research*, 18(2), 329–337.
Rizzetto, F. and Tosi, L., 2012. Rapid response of tidal channel networks to sea-level variations (Venice Lagoon, Italy). *Global and Planetary Change*, 92: 191–197.
Romine, B.M.; Fletcher, C.H.; Frazer, L.N.; Genz, A.S.; Barbee, M.M., and Lim, S.C., 2009. Historical shoreline change, southeast Oahu, Hawaii; applying polynomial models to calculate shoreline change rates. *Journal of Coastal Research*, 25(6), 1236–1253.

Schwimmer, R.A., 2001. Rates and processes of marsh shoreline erosion in Rehoboth Bay, Delaware, USA. *Journal of Coastal Research*, 17(3), 672–683.
Seminara, G., 2006. Meanders. *Journal of Fluid Mechanics*, 554, 271–297.
Shalowitz, A.L., 1964. *Shore and Sea Boundaries*. V1, Publication 10-1. Washington D.C.: U.S. Department of Commerce, Coast and Geodetic Survey, 420p.
Sharma, S.; Goff, J.; Moody, R.M.; McDonald, A.; Byron, D.; Heck, K.L., Jr.; Powers, S.P.; Ferraro, C., and Cebrian, J., 2016. Effects of shoreline dynamics on saltmarsh vegetation. *PLoS ONE*, 11(7), 1–14.
Strahler, A.N., 1957. Quantitative analysis of watershed geomorphology. *Eos, Transactions American Geophysical Union*, 38(6), 913–920.
Taddia, Y.; Stecchi, F., and Pellegrinelli, A., 2019. Using DJI phantom 4 RTK drone for topographic mapping of coastal areas. International Archives of the Photogrammetry, Remote Sensing and Spatial Information Sciences, Volume XLII-2/W13, 625–630.
Wadsworth, J.R., 1980. Geomorphic characteristics of tidal drainage networks in the Dublin River system, Sapelo Island, GA. Athens, Georgia: University of Georgia, Ph.D. dissertation.
Weber, A.H. and Blanton, J.O., 1980. Monthly mean wind fields for the Southern Atlantic Bight. *Journal of Physical Oceanography*, 10, 1256–1263.
Wallace, K.J.; Callaway, J.C., and Zedler, J.B., 2005. Evolution of tidal creek networks in a high sedimentation environment: A 5-year experiment at Tijuana Estuary, California. *Estuaries*, 28(6), 795–811.
Wilson, C.A.; Hughes, Z.J.; FitzGerald, D.M.; Hopkinson, C.S.; Valentine, V., and Kolker, A.S., 2014. Saltmarsh pool and tidal creek morphodynamics: Dynamic equilibrium of northern latitude saltmarshes. *Geomorphology*, 213, 99–115.